Hindered Transport of Spherical Macromolecules in Fibrous Membranes and Gels

Methods are described for calculating the effects of hydrodynamic interactions on the hindered transport of solid spherical macromolecules in ordered or disordered fibrous media. These methods are applied to a medium made up of a square lattice of straight, bead-and-string-type fibers. Hydraulic permeabilities and coefficients governing hindered diffusion and convection are obtained from a detailed hydrodynamic model, and the hindered transport coefficients are shown to be in very good agreement with an effective medium approach based on Brinkman's equation. The use of Brinkman's equation for the calculation of hindered transport rates in fibrous membranes and gels is validated further by comparing with experimental data from the literature.

R.J. Phillips
W.M. Deen
Department of Chemical Engineering
Massachusetts Institute of Technology
Cambridge, MA 02139

J.F. Brady
Chemical Engineering
California Institute of Technology
Pasadena, CA 91125

Introduction

Transport of macromolecules through pores of molecular dimensions is usually much slower than in bulk solution. Steric and sometimes long-range interactions between a permeating macromolecule and the solid phase prevent free access to the entire fluid volume in a pore, and hydrodynamic interactions reduce the macromolecule's mobility. The objective of theories of hindered transport (Deen, 1987) is to relate the values of transport coefficients to the size, shape and other fundamental properties of the solute and the porous medium. This information would enable one to predict the ability of a porous material of known microstructure to separate a given mixture of macromolecules or, alternatively, to infer structural characteristics of the porous material or macromolecules from measured transport rates.

The usual approach in hydrodynamic models of hindered transport has been to represent the porous medium as an assemblage of straight, cylindrical pores. However, many real systems, including gels and a variety of membranes, more closely resemble arrays of fibers with fluid-filled interstices. For these materials, the precise meaning of model parameters such as pore radius is unclear, because the connection between the model geometry and the actual microstructure is at best tenuous. It would, therefore, be of great value to develop a theoretical model based on the same physical concepts that have been applied successfully to straight pores, but which specifically accounts for a fibrous microstructure.

Previous attempts to model hindered transport in fibrous systems have had some success in correlating experimental data (Ogston et al., 1973; Curry and Michel, 1980; Peppas and Reinhart, 1983), but have not evaluated the effects of the hydrodynamic interactions between the fibers and the diffusing macromolecule. Thus, while steric exclusion of macrosolutes by arrays of fibers has been treated in some detail (Ogston, 1958; Fanti and Glandt, 1989), there is little information on the increased drag on a macromolecule in a fibrous medium. For cylindrical or slit-like pores, steric and hydrodynamic contributions to solute hindrances are of comparable importance (Deen, 1987), suggesting that hydrodynamic interactions in fibrous media should not be ignored.

In this paper, we describe two approaches for calculating transport coefficients for a spherical macromolecule in a matrix of fibers. The first method is an effective medium approach that makes use of Brinkman's equation. In the second calculation, what has been called the "Stokesian-dynamics" method (Brady et al., 1988) is used to calculate *local* hydrodynamic coefficients at any position in a fibrous bed. These local coefficients describe transport over time scales so short that a mobile macromolecule does not move a distance comparable to its own radius and are therefore not appropriate for calculating a macroscopic flux through a membrane or gel. However, local coefficients can be used in conjunction with dynamic simulations (Brady and Bossis, 1988) or with generalized Taylor dispersion theory (Brenner

Correspondence concerning this paper should be addressed to W. M. Deen.

and Adler, 1982) to calculate *global* transport coefficients that do describe diffusion and convection over macroscopic length scales. In this work the theory of Brenner and Adler is used to obtain numerical results for the hindered transport coefficients governing the motion of a spherical macromolecule with radius a through an infinite, square lattice of fibers, also of radius a. These results, along with experimental data from the literature, are then used to examine the applicability of Brinkman's equation to hindered transport in fibrous media.

Theory

Effective medium approach

The macroscopic flux J^* of probability density $\bar{P}$ through an effective medium can be described by the equation

$$J^* = -\underline{\underline{D}}^* \cdot \nabla \bar{P} + U\bar{P}. \tag{1}$$

Here $\underline{\underline{D}}^*$ is the dispersion tensor for the effective medium and U^* is the solute velocity. The overbar on the probability density indicates that this is a macroscopic probability density. It is the volume average of the local probability density P over a length scale large enough to represent the microstructure of the porous medium. For a spatially periodic porous medium, the appropriate length scale for averaging is the dimension of a single unit cell. Thus, $\bar{P}$ varies over a length scale which is large compared to that of a unit cell. For an isotropic medium, the dispersion tensor in Eq. 1 is just the product of the effective dispersion coefficient D^* and the identity tensor. From the Stokes-Einstein equation one knows that this effective dispersion coefficient D^* is equal to k_BT/f, where k_BT is the product of Boltzmann's constant and absolute temperature, and f is the friction coefficient equal to $6\pi\mu a$ for a sphere of radius a in a pure fluid with viscosity μ.

For the case considered here, the value of f can be determined by using Brinkman's equation (Brinkman, 1947) for flow in a porous medium:

$$\mu\nabla^2 v - \nabla p = (\mu/k)v. \tag{2}$$

Here p is pressure and v is the velocity averaged over both the fluid and the fiber phases. Equation 2 can be seen as Stokes' equations with an additional term to account for the force exerted on the fluid by the fibers or, alternatively, it can be seen as Darcy's law with an additional term that accounts for viscous stresses in the fluid phase. The only structural information included in this effective medium model is contained in k, the hydraulic permeability.

The value of f obtained by solving Eq. 2 subject to no-slip boundary conditions at the sphere surface and constant velocity far from the sphere center is (Brinkman, 1947; Howells, 1974)

$$\frac{f}{6\pi\mu a} = 1 + (a^2/k)^{1/2} + \frac{1}{3}(a^2/k). \tag{3}$$

Thus, from the Stokes-Einstein equation, one would expect

$$\frac{D^*}{D_o} = \frac{1}{1 + (a^2/k)^{1/2} + \frac{1}{3}(a^2/k)} \tag{4}$$

for the effective medium, where D_o is the diffusivity in pure fluid. For a force-free particle, Brinkman's equation would require that the particle velocity U^* be equal to the velocity v averaged over both the fiber and fluid phases. However, for a particle that cannot access positions in the fiber phase, a better approximation can be obtained by equating U^* with the average velocity of the fluid phase only. Thus, for a medium with volume fraction ϕ, one expects

$$U^* = \frac{v}{1 - \phi}, \tag{5}$$

and both quantities required to evaluate the flux using Eq. 1 are known. The hydraulic permeability k can be measured directly in many cases. It can also be determined theoretically for certain fiber geometries (Hasimoto, 1959; Spielman and Goren, 1968) or can be evaluated using well-known, semiempirical correlations (Jackson and James, 1986).

The result given by Eq. 3 can be derived rigorously for a medium consisting of a dilute, disordered array of hard spheres (Childress, 1972; Howells, 1974; Hinch, 1977; Freed and Muthukumar, 1978). Although one might expect that the details of a fibrous vs. a hard-sphere microstructure might not be important for small enough volume fractions, it is not at all clear that this will be true for volume fractions of interest for hindered transport. Further examination of Eqs. 4 and 5 is therefore required before passing judgment as to their value.

Calculation of Local Transport Coefficients

To improve upon the effective medium approach, one requires a method for calculating the enhanced resistance to transport caused by hydrodynamic interactions between the solute macromolecule and the fibers. The details of the method used to calculate these interactions are presented elsewhere (Brady et al., 1988) and thus will not be repeated here. It will, however, be worthwhile to briefly outline the general approach.

One begins by specifying the locations of N spherical particles within a periodic unit cell. The spheres can be distributed in any configuration that is desired. For the hindered transport problem being studied here, it is most convenient to align N-1 of the spheres in rows to model fibers and let one sphere model the diffusing macromolecule, which wanders randomly under the influence of Brownian motion. For conditions where the particle Reynolds number is small, the forces on the N particles can be related by

$$F = \mathcal{R} \cdot (U - v). \tag{6}$$

Here F and U are vectors of dimension $3N$ containing the forces and velocities of the particles, respectively. The vector v is, again, the average velocity. The $3N \times 3N$ matrix $\mathcal{R}$ is the grand resistance matrix and relates the vector quantities as shown in Eq. 6.

An accurate approximation to $\mathcal{R}$ can be obtained by separating the hydrodynamic interactions into far-field and near-field components. The far-field, or long-range interactions are calculated in terms of an expansion in moments of the force density on each particle surface about its center and, in principle, can be carried out to any level of accuracy that is desired. These far-field interactions decay very slowly, and so in an infinite

medium an accelerated convergence scheme known as the Ewald summation technique is used in their evaluation. Using this technique allows one to properly "renormalize" the far-field interactions as well as sum them in a computationally-efficient manner. The level of these interactions accounted for in this work corresponds with what is termed the "F method" in Phillips et al. (1988a, b) or, alternatively, what is termed the "Ewald sum of the Rotne-Prager tensor" in Beenakker (1986). This level of accuracy accounts for far-field interactions up to $O(1/r^3)$, where r refers to the distance between two spheres. It is important to note, however, that including higher moments to the level termed the "F-T-S method" by Phillips et al., or up to $O(1/r^6)$, did not alter the results to be presented below by more than 2-3%. There is a subtle difference between the term "F method" as used here and that used in Phillips et al. Whereas the near-field or lubrication contributions referred to in Phillips et al. do not include torque and stresslet interactions, those interactions were included in the near-field terms used here.)

The near-field or short-range interactions are accounted for in a pairwise additive fashion. In other words, the short-range interactions between two spheres are calculated under the assumption that the effects of the other N-2 spheres in the periodic unit cell are negligible. These calculations are accomplished using the exact two-sphere results in the literature (Jeffrey and Onishi, 1984; Kim and Mifflin, 1985). Addition of the far-field and near-field contributions gives the complete approximation to the grand resistance matrix of Eq. 6. This approach to forming the grand resistance matrix has been tested previously for both ordered and disordered arrays of spheres and has been found to agree well with the existing body of theoretical and experimental results (Brady et al., 1988; Phillips et al., 1988a, b).

Local transport properties governing particle motion may be derived directly from $\mathcal{R}$. Following Brenner and Adler (1982), one can define a local flux $\boldsymbol{J}$ of probability density P at any point in the unit cell of a spatially-periodic lattice by

$$\boldsymbol{J} = -\underset{\approx}{D} \cdot \nabla P + \boldsymbol{U}P, \tag{7}$$

where P is a function of position $\boldsymbol{X}$ and the time since the diffusing macromolecule was released at some particular position. The terms $\underset{\approx}{D}$ and $\boldsymbol{U}$ are the local dispersion coefficient and local velocity of the tracer macromolecule, respectively. The probability density P is normalized such that its integral over all space, including the fluid and solid phases of all unit cells, is unity.

The quantities $\underset{\approx}{D}$ and $\boldsymbol{U}$ are obtained by partitioning the grand resistance matrix into submatrices of dimension 3 × 3, where each submatrix $\underset{\approx}{R}^{ij}$ relates the force on particle i to the velocity of particle j relative to the average velocity $\boldsymbol{v}$. If the ith sphere models a macromolecule diffusing in a stagnant fluid ($\boldsymbol{v} = \boldsymbol{0}$) and all of the other spheres are immobile, then the force and velocity of the one mobile sphere are related by

$$\mathbf{F}^i = \underset{\approx}{R}^{ii} \cdot \boldsymbol{U}^i. \tag{8}$$

Thus, applying the generalized form of the Stokes-Einstein equation, one obtains

$$\underset{\approx}{D} = kT(\underset{\approx}{R}^{ii})^{-1}. \tag{9}$$

Similarly, consideration of a system with average velocity $\boldsymbol{v}$ yields

$$\boldsymbol{U}^i = [(\underset{\approx}{R}^{ii})^{-1} \cdot \sum_{j=1}^{N} \underset{\approx}{R}^{ij}] \cdot \boldsymbol{v} \tag{10}$$

for the velocity of a force-free particle i. The coefficients given by Eqs. 8 and 10 are not exact, as there is an error associated with the periodic boundary conditions used in modeling the infinite system. Essentially this error is derived from the fact that properties such as the average velocity $\boldsymbol{v}$, which are specified in Eqs. 8 and 10 for the infinite medium as a whole, must actually be satisfied in each periodic unit cell if all of the unit cells are to be identical. This error alters the erms in $\mathcal{R}$ by an amount that is $O(1/N)$ and is discussed in some detail by Durlofsky and Brady (1987).

Calculation of Global Transport Coefficients

It now remains to relate the local coefficients of Eq. 7 to global coefficients, which describe transport on a macroscopic length scale (i.e., over many periodic unit cells). The global transport coefficients D^* and U^* of Eq. 1, distinguished from the coefficients in Eq. 7 by the asterisk, can be evaluated using generalized Taylor dispersion theory. As this theory is quite involved and has been presented elsewhere (Brenner and Adler, 1982), only the relevant equations and definitions of the appropriate variables will be presented here.

If, as is the case here, one is studying a fibrous medium that is periodic on the length scale of a unit cell, then one can write the position vector $\boldsymbol{X}$ as the sum of global and local variables,

$$\boldsymbol{X} = \boldsymbol{X}_n + \boldsymbol{r}, \tag{11}$$

where $\boldsymbol{X}_n$ identifies a particular unit cell and $\boldsymbol{r}$ specifies a position within that unit cell. By summing the probability density in all of the unit cells, one calculates P_o, where

$$P_o(\boldsymbol{r}, t \mid \boldsymbol{r}') = \sum_n P(\boldsymbol{X}_n - \boldsymbol{X}'_n, \boldsymbol{r}, t \mid \boldsymbol{r}'). \tag{12}$$

Physically, $P_o(\boldsymbol{r}, t|\boldsymbol{r}')$ is the probability of finding the diffusing macromolecule at a particular position $\boldsymbol{r}$ in *any* of the unit cells at some time t, given that it was at a position $\boldsymbol{r}'$ at time $t = 0$. The sum over n in Eq. 12 is a sum over all the unit cells in space. One can eliminate the time-dependence of P_o by restricting the analysis to long times and using as a probability density P_o^∞, where

$$P_o^\infty(\mathbf{r}) = \lim_{t \to \infty} P_o(\boldsymbol{r}, t|\boldsymbol{r}'). \tag{13}$$

The probability density $P_o^\infty(\boldsymbol{r})$ represents the probability of finding the diffusing macromolecule at some local position $\boldsymbol{r}$ after it has had enough time to achieve steady state with respect to transport over the length scale of a unit cell, but not over the global or macroscopic length scale. It can be shown that the asymptotic approach to steady state is exponentially rapid with time (Brenner and Adler, 1982).

The equation governing P_o^∞ is

$$\nabla \cdot (\boldsymbol{U}P_o^\infty) - \nabla \cdot \underset{\approx}{D} \cdot \nabla P_o^\infty = 0, \tag{14}$$

with the boundary conditions

$$[\![P_o^\infty]\!] = 0 \text{ and } [\![\nabla P_o^\infty]\!] = 0 \tag{15}$$

on boundaries of the unit cell in the fluid phase and

$$\boldsymbol{n} \cdot (\boldsymbol{U}P_o^\infty - \underset{\approx}{D} \cdot \nabla P_o^\infty) = 0 \tag{16}$$

on the solid surfaces and the normalization condition

$$\int_{r_o} P_o^\infty \, d\boldsymbol{r} = 1. \tag{17}$$

In Eq. 15 the symbol $[\![\ ]\!]$ denotes the difference between the values of the argument at geometrically-equivalent positions on opposite faces of a unit cell, and $\boldsymbol{n}$ is a unit normal vector pointing into the unit cell. The velocity $\boldsymbol{U}^*$ is given by

$$\boldsymbol{U}^* = \int_{r_o} (\boldsymbol{U}P_o^\infty - \underset{\approx}{D} \cdot \nabla P_o^\infty) \, d\boldsymbol{r}. \tag{18}$$

The integral over r_o in Eqs. 17 and 18 implies an integral over the volume of a unit cell in the periodic lattice. Note that setting P_o^∞ equal to a constant satisfies Eqs. 14, 15 and 16 if the average velocity is zero ($\boldsymbol{v} = \boldsymbol{0}$). In this case, the value of P_o^∞ is determined by Eq. 17, and the value of $\boldsymbol{U}^*$ given by Eq. 18 is just a spatial average of the local coefficient $\boldsymbol{U}$.

The result for $\underset{\approx}{D}^*$ is most conveniently expressed in terms of a vector field $\boldsymbol{B}$, defined by the solution to

$$\nabla \cdot (P_o^\infty \underset{\approx}{D} \cdot \nabla \boldsymbol{B}) - (\boldsymbol{U}P_o^\infty - \underset{\approx}{D} \cdot \nabla P_o^\infty) \cdot \nabla \boldsymbol{B} = P_o^\infty \boldsymbol{U}^*, \tag{19}$$

with boundary conditions

$$[\![\boldsymbol{B}]\!] = -[\![\boldsymbol{r}]\!] \text{ and } [\![\nabla \boldsymbol{B}]\!] = \boldsymbol{0} \tag{20}$$

on boundaries of the unit cell in the fluid phase and

$$\boldsymbol{n} \cdot \underset{\approx}{D} \cdot \nabla \boldsymbol{B} = \boldsymbol{0} \tag{21}$$

on the solid surfaces. The global dispersion coefficient, $\underset{\approx}{D}^*$, is then given by

$$\underset{\approx}{D}^* = \int_{r_o} (P_o^\infty (\nabla \boldsymbol{B})^t \cdot \underset{\approx}{D} \cdot \nabla \boldsymbol{B}) \, d\boldsymbol{r}, \tag{22}$$

where $(\nabla \boldsymbol{B})^t$ denotes the transpose of the tensor $\nabla \boldsymbol{B}$. The vector field $\boldsymbol{B}$, which one must evaluate in order to make use of Eq. 22, arises as a matter of mathematical convenience in the development of Brenner and Adler (1982) and is related to physical quantities by Koch *et al.* (1989).

Results and Discussion

The configuration of fibers chosen to model a fibrous bed is shown in Figure 1. Parallel, bead-and-string fibers aligned along the z axis were arranged in a square lattice in the x-y plane, with fiber-to-fiber spacing L and a gap spacing d separating the spheres of a given fiber. The dimensions L and d are made dimensionless by the sphere radius a. This configuration was selected because it seemed the simplest geometry which could yield meaningful results for the hindered transport problem.

Two-dimensional cross-sections of the square lattice of fibers

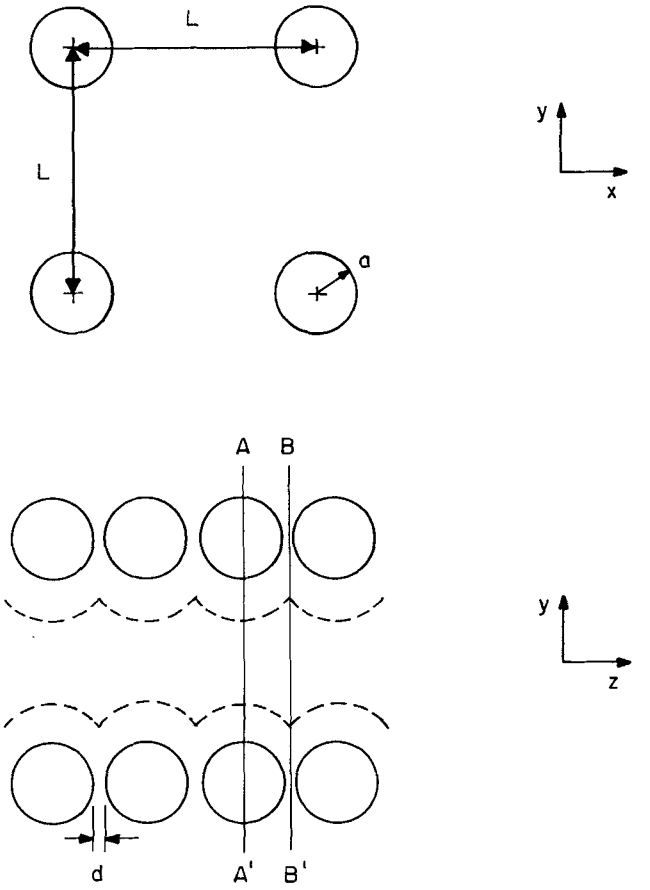

Figure 1. Top: two-dimensional cross-section of a periodic lattice of bead-and-string fibers.
Bottom: cross-sections AA′ and BB′ used in solving Eqs. 14 and 19.

Using either cross-section results in a two-dimensional lattice, but the gap between the fibers is larger for the BB′ cross-section than for the AA′ cross-section. The dashed curves bound the region accessible to a mobile sphere of radius a.

were taken at the positions denoted by the lines AA′ and BB′ in Figure 1 (lower), and Eqs. 14 and 19 were solved for each of these two cross-sections by neglecting the true three-dimensional nature of the bead-and-string fibers. In other words, once the local coefficients were obtained for the AA′ and BB′ cross-sections, Eqs. 14 and 19 were solved assuming the fibers were cylinders of constant radius aligned in the z direction. The difference between these two cross-sections is that a diffusing macromolecule can sample a higher fraction of the total area in the cross-section taken at BB′ than in that taken at AA′. These differences can be minimized by choosing d to be a small fraction of the fiber radius. A value of $d = 0.05$ was used in this work. One would expect the actual result for a matrix of such fibers to lie between the two results obtained in this manner. Thus, when the transport properties calculated from the two cross-sections differed by more than about 2%, the average of the two results is reported and the range of results is given by the error bars shown.

Equations 14 and 19 were solved using a Galerkin finite element method with bilinear basis functions (Finlayson, 1980). The choice of a finite element method of solution is particularly convenient in this problem because of the form of the boundary

conditions (Eqs. 16 and 21). For a finite-sized solute molecule, $\underline{\underline{D}}$ and $\boldsymbol{U}$ are identically zero on solid surfaces, and thus it is difficult to specify any properties of $\boldsymbol{P}$ and $\boldsymbol{B}$ other than that they and their gradients must be finite. The advantage of the finite element approach is that specific statements regarding the behavior of $\boldsymbol{P}$ and $\boldsymbol{B}$ are not required. Rather, one applies the conditions of no flux on the solid surfaces in precisely the form given in Eqs. 16 and 21, and thus the proper physical requirement of no flux into the fibers is easily incorporated into the method of solution.

The size of the periodic unit cell used to calculate the hydrodynamic interactions was not the same as the size of the periodic unit cell used in the Taylor dispersion calculations (i.e., in solving Eqs. 14 and 19). For the latter, we employed the smallest possible unit cell dimension, L. However, as discussed previously, there is an $O(1/N)$ error in the terms of $\mathcal{R}$ caused by the use of periodic boundary conditions in modeling the infinite system. It is therefore necessary to choose a large enough periodic unit cell (i.e., a large enough value of N) to make this error in the calculation of the local coefficients negligible. In this work, $\underline{\underline{D}}$ and $\boldsymbol{U}$ were obtained using a unit cell of nine fibers, each containing ten spheres aligned in the z direction. The results were not changed by more than 2–3% when unit cells with 16 fibers or with 15 spheres per fiber were used, indicating that artifacts arising from periodic images were not important in these calculations. The calculations were done on a CYBER 205 supercomputer. A typical configuration required the evaluation of local coefficients at about 500 positions, which used about 30 minutes of CPU time. The computer time required to solve Eqs. 14 and 19 was negligible compared to the time required to calculate the local coefficients.

Comparison of Theoretical Predictions

In Figures 2 and 3 drag coefficients and hydraulic permeabilities for flow in the x or y directions through a square lattice of fibers are shown. These results were obtained by noting that, for a periodic unit cell in which no solute macromolecule is present (i.e., all the spheres are part of the bead-and-string fibers), the drag coefficient for any one of the N identical spheres is given by (Phillips et al., 1988b)

$$f = \sum_j R_{xx}^{ij} \tag{23}$$

where i can be any number from 1 to N since all the spheres are equivalent. The subscript xx refers to the fact that the drag in the x direction due to flow in the x direction is being considered. The value of f can be related to k by

$$k = \frac{\mu}{fn}, \tag{24}$$

where n is the number density of spheres. Also plotted in Figures 2 and 3 are the theoretical results of Hasimoto (1959) who calculated the permeability of a square lattice of straight, cylindrical fibers in creeping flow. The good agreement between the two sets of results underscores both the validity of our approximation for $\mathcal{R}$ and the hydrodynamic similarity of the bead-and-string and cylindrical rod models of fibers.

Although the parameter L used in Figures 2 and 3 is useful for describing square lattices of fibers, for other geometries it is often convenient to use the volume fraction of fibers ϕ. For a square lattice of bead-and-string fibers such as that shown in Figure 1, ϕ and L are related by

$$\phi = \frac{\frac{4}{3}\pi}{(2+d)L^2} \tag{25}$$

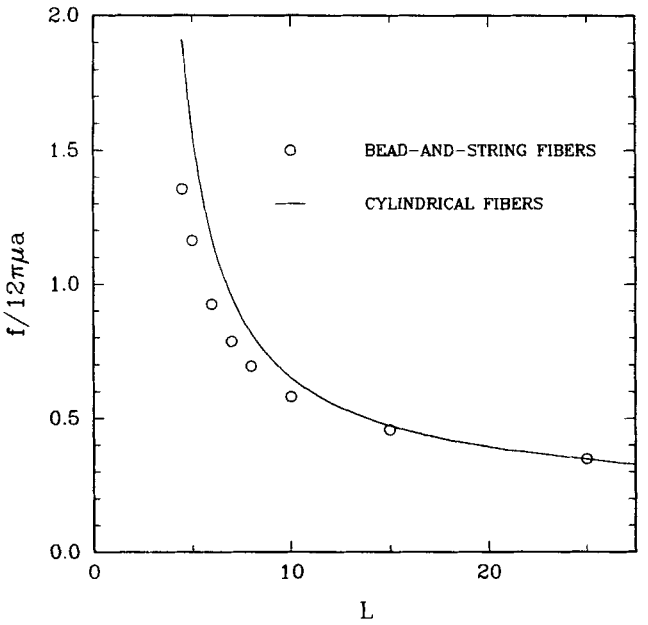

Figure 2. Dimensionless friction factor $f/12\pi\mu a$ vs. L for bead-and-string fibers (Eq. 24) and cylindrical fibers (Hasimoto, 1959).

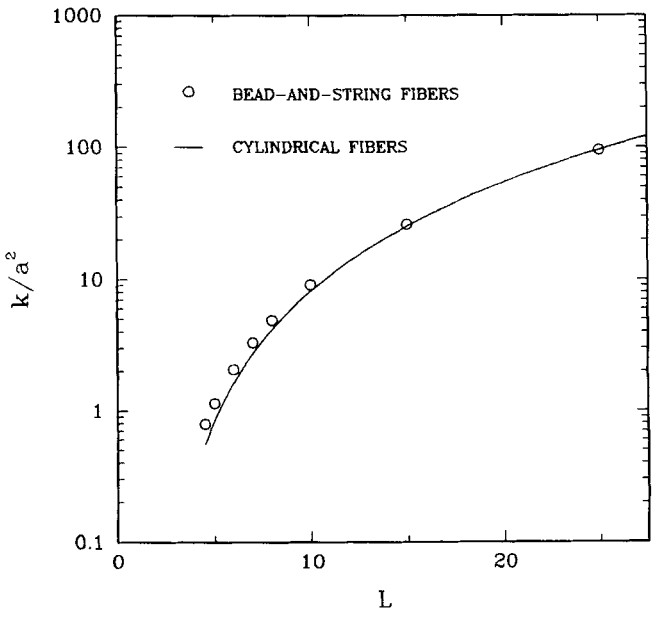

Figure 3. Dimensionless permeability k/a^2 (Eq. 24) vs. L for bead-and-string fibers and cylindrical fibers.

whereas for a square lattice of smooth, cylindrical fibers

$$\phi = \frac{\pi}{L^2}. \tag{26}$$

Thus, a given value of ϕ will correspond to different values of L for the two types of fibers. Nonetheless, when the results of Figures 2 and 3 are replotted as a function of ϕ, the agreement between the bead-and-string and smooth cylinder models remains good. For most fibrous systems, the volume fraction is more readily obtained than the interfiber spacing, and thus the remaining results of this section will be presented as a function of ϕ rather than L.

In Figure 4, values of the dispersion coefficient are shown for a spherical macromolecule with the same radius as the fibers diffusing in a medium with no flow ($v = 0$). The scalar coefficient D^*_{xx} is the component of $\underset{\approx}{D}^*$ that governs dispersion in the x direction due to a probability density gradient in the x direction. For this periodic system, D^*_{yy} will equal D^*_{xx}, while D^*_{xy} and D^*_{yx} will be zero. The Stokes-Einstein diffusivity is denoted by D_o, and the volume fraction of fibers is given by ϕ. The calculations were done both with and without near-field interactions.

The solid curve in Figure 4 is the Brinkman or effective medium result, obtained using Eq. 4 together with hydraulic permeabilities calculated from Eq. 24. The Brinkman results and the generalized Taylor dispersion results are in remarkably good agreement, especially when near-field interactions are neglected. This observation is consistent with the expectation that

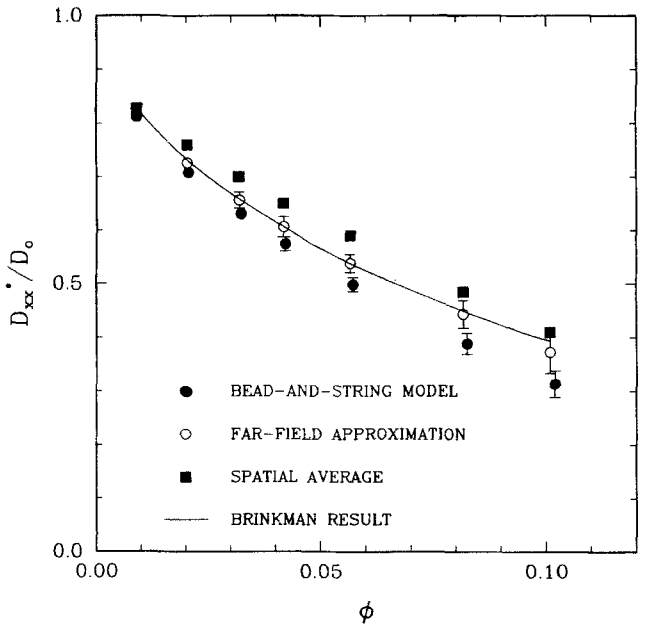

Figure 4. Dimensionless, global dispersion coefficient D^*_{xx}/D_o vs. volume fraction ϕ.

Solid circles denote the result obtained from Eq. 22 using local coefficients calculated from the complete approximation to the grand resistance matrix. Open circles show results obtained using coefficients calculated from the far-field approximation to the grand resistance matrix, while solid squares represent the spatial average of local coefficients that do include near-field interactions. The solid curve is the result predicted by Brinkman's equation (Eq. 4) using the hydraulic permeabilities for bead-and-string fibers in Figure 3. The limits of the error bars are the results obtained by using the AA′ and BB′ cross-sections in Figure 1.

Brinkman's equation should become more accurate for dilute systems, where far-field interactions dominate. Indeed, Durlofsky and Brady (1987) demonstrated that the rate of decay of far-field hydrodynamic interactions evaluated using the Stokesian dynamics method corresponds closely to the prediction of Brinkman's equation. Including the near-field interactions caused a deviation of about 20% from the Brinkman results at the maximum volume fraction studied, $\phi = 10.1\%$, which corresponds to $L = 4.5$. (From Figure 1, macroscopic transport in the x and y directions ceases for $L < 4$, or $\phi > 12.8\%$, for the AA′ cross-section.) The close correspondence between the Brinkman results and those of the more detailed hydrodynamic model suggests that the hydraulic permeability k embodies the principal effects of the fibers on diffusion, as well as their effect on solvent flow. In other words, the details of the shape and arrangement of the individual fibers appear to be only of secondary importance in determining hindrances to diffusive transport of a macromolecular solute.

The solid squares in Figure 4 are the results obtained by neglecting the effects predicted by generalized Taylor dispersion theory and simply spatially averaging the local coefficient $\underset{\approx}{D}$ given in Eq. 9. The values obtained in this manner differ significantly from the Brinkman prediction, and even more so from the more rigorous calculation involving Eqs. 18 and 22. That one should not expect the spatial average of $\underset{\approx}{D}$ to be the same as $\underset{\approx}{D}^*$ can be seen clearly by considering the case where a mobile solute is trapped inside a "cage" of surrounding fibers. For the periodic system under consideration here, such a condition could be achieved by setting $L = 4$ using the AA′ cross-section of Figure 1. Because the solute is not able to escape from its "cage," the global dispersion coefficient $\underset{\approx}{D}^*$ must be zero. However, the local dispersion coefficient $\underset{\approx}{D}$ is still finite everywhere except on the lines connecting the fiber centers, and thus the spatial average of $\underset{\approx}{D}$ is nonzero. Only by properly solving Eq. 14 and 19 can the correct global coefficients be obtained. This simple example illustrates the important distinction between local and global coefficients.

In Figure 5, values of U^*_x/v_x are plotted as a function of volume fraction for the limiting case where $v_x \to 0$. Again, both the far-field and the complete results are plotted. The solid curve is the average fluid velocity given by Eq. 5. Note that the particle velocity should not be expected to equal the average fluid velocity, even for small ϕ. This is because the finite size of the particle prevents it from sampling regions near solid boundaries, where the fluid velocity is lowest. The far-field approximation tends to overestimate U^*_x by a significant amount. The result obtained from Eq. 5 underestimates it up to volume fractions of about $\phi = 5\%$, after which point the hindering effect of the fibers causes the particle velocity to fall below the average fluid velocity. Note that this qualitative behavior must be obtained in order for macroscopic transport to cease at $L = 4$ (for the AA′ cross-section). The overall effects of the fibers on convective solute transport are seen to be relatively small over the volume fractions studied, the values of U^*_x/v_x from Eq. 18 never deviating more than 10% from unity.

The results shown in Figures 4 and 5 are valid in the limit of low Peclet number, $Pe = v_x a/D_o \to 0$. For nonzero Pe, the probability distribution P^∞_o in Eq. 14 changes, and thus, in principle, both D^*/D_o and U^*_x/v_x can change also. In Figure 6, D^*/D_o is plotted vs. Pe for various values of ϕ. As seen in many other systems, the dispersion coefficient increases with increasing Peclet

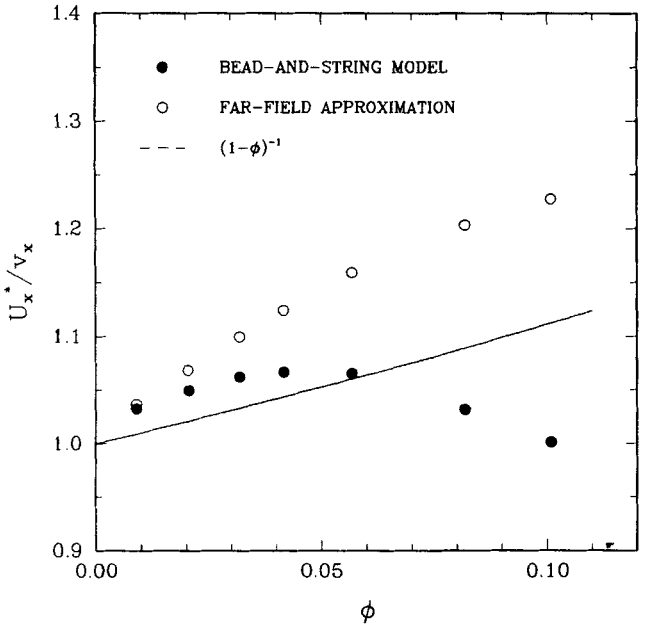

Figure 5. Dimensionless velocity U_x^* vs. volume fraction ϕ.

Solid circles and open circles are analagous to those in Figure 4 and show the results obtained from Eq. 18 using the complete and far-field approximation to the grand resistance matrix, respectively. The solid line is the average fluid velocity given by Eq. 5.

most applications, even where convection contributes appreciably to the macroscopically observable transport, this "microscopic" Peclet number will be exceedingly small, and the effect of Pe on D_{xx}^* will be negligible (Deen, 1987). The dependence of U_x^*/v_x on Pe did not significantly alter the results shown in Figure 5 over the range of Pe considered ($Pe \leq 1$).

Comparison with Experiment

Calculations involving the more rigorous bead-and-string model are rather involved and therefore have only been carried out for a square lattice of fibers having the same radius as the solute macromolecule. However, the results predicted by Brinkman's equation, which agreed closely with the more rigorous theory, can be readily applied to any fibrous system for which the hydraulic permeability is known. Indeed, the good agreement between these two approaches suggests that the effective medium model may be a very useful one for fibrous systems in general. It is therefore of interest to compare the predictions of Eq. 4 with experimental data taken from the literature.

Laurent and Pietruszkiewicz (1961) and Laurent et al. (1963) measured the sedimentation rates, and hence friction coefficients, of several proteins in hyaluronic acid solutions. Hydraulic permeabilities for hyaluronic acid solutions have been measured by several research groups, and the results are summarized by Ethier (1986). In Figure 7, the results predicted using Eq. 4 together with the experimentally-measured hydrau-

number. In interpreting Figure 6 it is important to note that the length scale used in the Peclet number is the fiber radius. In

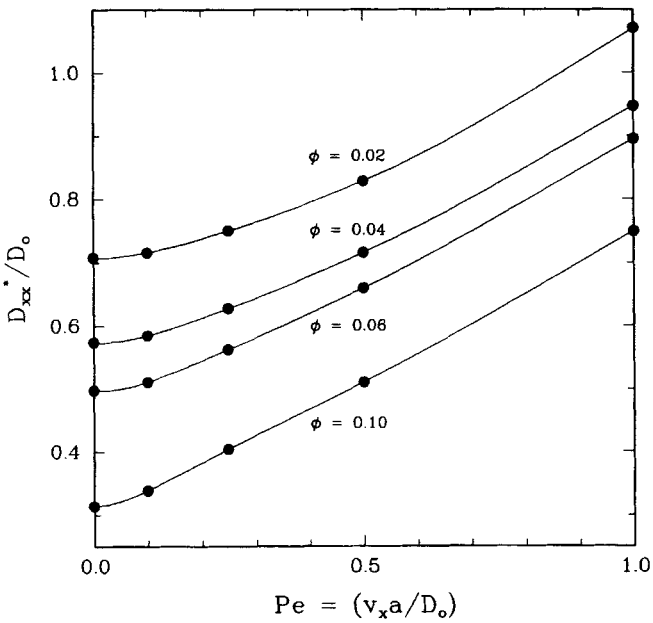

Figure 6. Dimensionless, global dispersion coefficient D_{xx}^*/D_o vs. Peclet number Pe for volume fractions ranging from $\phi = 0.02$ ($L = 10.0$) to $\phi = 0.10$ ($L = 4.5$).

Although error bars have been left off for clarity, they are comparable in size or smaller than those shown in Figure 4 for the corresponding volume fraction.

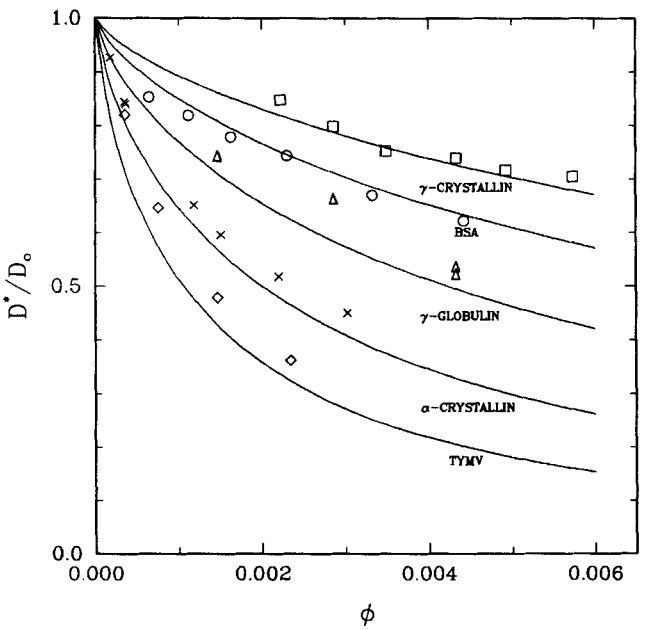

Figure 7. Dimensionless dispersion coefficients measured experimentally for proteins in hyaluronic acid solution (Laurent and Pietruszkiewicz, 1961; Laurent et al. 1963) vs. values predicted by Brinkman's equation.

Hyaluronic acid with a molecular weight of 1.7×10^6 was used in obtaining these data. The macromolecules used and their Stokes-Einstein radii (r_s) are γ-crystallin (r_s = 23.5 Å), bovine serum albumin (r_s = 34 Å), human and bovine γ-globulin (r_s = 56 Å), α-crystallin (r_s = 97 Å), and turnip yellow mosaic virus (r_s = 155 Å). Experimental data obtained from Ethier (1986) were used in Eq. 4 to obtain the values predicted by Brinkman's equation.

lic permeability data are compared with the experimental results for D^*/D_o. In generating the solid curves, the sphere radius a in Eq. 4 was assumed to equal the Stokes-Einstein radii r_s of the proteins. As shown in Figure 7, theory and experiment agree to within about 2–3% for the γ-crystallin and bovine serum albumin measurements, and to within 10% for the human γ-globulin, α-crystallin, and turnip yellow mosaic virus measurements. Remarkably, no adjustable parameters were needed to obtain this excellent agreement between theory and experiment. In addition, the only structural information required was the Stokes-Einstein radius of the diffusing macromolecules and the hydraulic permeability of the hyaluronic acid medium. Such information is readily available for many systems of interest. Thus, the simplicity and accuracy of the effective medium model suggest that it could be of great use in predicting rates of hindered transport through fibrous membranes and gels used in both physiological and industrial processes.

Conclusions

From the evidence presented here, it should be clear that hydrodynamic interactions play a very important role in determining the rates of macromolecular transport in fibrous membranes and gels. Two approaches to calculating the effects of these interactions were discussed. The first, and simpler, method was an effective medium approach that made use of Brinkman's equation. The second calculation involved choosing a particular fiber geometry and ratio of solute to fiber radius and rigorously evaluating the global transport properties using the Stokesian dynamics method together with generalized Taylor dispersion theory. For the case considered here, the effective medium approach gave results that agreed well with the more rigorous calculation. This good agreement has yet to be tested for different ratios of solute to fiber radius and for different fiber geometries. It still is encouraging to find that the theoretical evidence tends to validate the use of Brinkman's equation for this calculation. It suggests that, in many cases, the only structural information one may need to predict rates of hindered transport in fibrous systems is contained in the hydraulic permeability, which can often either be measured by a single experiment or be estimated by well-known correlations.

Having tested the effective medium approach theoretically, its predictions were compared with experimental data from the literature for a case where both diffusion and hydraulic permeability data were available. Even with no adjustable parameters employed in the theoretical calculations, the agreement between theory and experiment was excellent. However, it must be emphasized that, although the hydrodynamic interactions included in the Brinkman model clearly play a significant role in hindered transport, one should not conclude that other factors can be safely neglected in all cases. Fiber geometry, fiber flexibility, and electrostatic effects, among others, might all play an important role under certain conditions. Further research will be required to determine how these factors combine to determine overall rates of hindered transport in fibrous membranes and gels.

Acknowledgment

This work was supported by a grant from the National Institutes of Health (DK 20368) and a grant of supercomputer time from the John von Neumann Center, Princeton, N.J. R.J. Phillips is the recipient of a fellowship from the National Science Foundation.

Notation

a = sphere radius
$\boldsymbol{B}$ = vector-field used in evaluating global coefficients
d = gap spacing between spheres in bead-and-string fibers
D_o = diffusion coefficient in bulk solution
$\underset{\approx}{D}$ = local dispersion tensor
$\underset{\approx}{D}^*$ = mean or global dispersion tensor
f = friction coefficient
$\boldsymbol{F}$ = force vector
$\boldsymbol{J}$ = flux of probability density
$\boldsymbol{J}^*$ = mean or macroscopic flux of probability density
k = hydraulic permeability
k_B = Boltzmann's constant
L = interfiber spacing
$\boldsymbol{n}$ = unit normal vector
N = number of spheres in a periodic unit cell
P = probability density
Pe = Peclet number based on fiber radius
P_o = probability density summed over all unit cells
P_o^∞ = long-time limit of P_o
r = distance between two spheres
$\boldsymbol{r}$ = position inside a unit cell
$\mathcal{R}$ = grand resistance matrix
$\underset{\approx}{R}^{ij}$ = 3×3 matrix component of $\mathcal{R}$, relating force on particle i to velocity of particle j
t = time
T = temperature
U = particle velocity
U^* = mean or global particle velocity
$\boldsymbol{U}^i$ = velocity of particle i
$\boldsymbol{v}$ = velocity averaged over fluid and fiber phases
$\boldsymbol{X}$ = position vector
$\boldsymbol{X}_n$ = position of nth unit cell
x, y, z = cartesian coordinates

Greek letters

ϕ = volume fraction of fibers
μ = fluid viscosity

Literature Cited

Beenakker, C. W. J., "Ewald Sum of the Rotne-Prager Tensor," *J. Chem. Phys.*, **85,** 1581 (1986).
Brady, J. F., and G. Bossis, "Stokesian Dynamics," *Ann. Rev. Fluid Mech.*, **20,** 111 (1988).
Brady, J. F., R. J. Phillips, J. C. Lester, and G. Bossis, "Dynamic Simulation of Hydrodynamically Interacting Suspensions," *J. Fluid Mech.*, **195,** 257 (1988).
Brenner, H., and P. M. Adler, "Dispersion Resulting from Flow through Spatially Periodic Media: II. Surface and Intraparticle Transport," *Phil. Trans. R. Soc. Lond. A,* **307,** 149 (1982).
Brinkman, H. C., "A Calculation of the Viscous Force Exerted by a Flowing Fluid in a Dense Swarm of Particles," *Appl. Sci. Res. A,* **1,** 27 (1947).
Childress, S., "Viscous Flow Past a Random Array of Spheres," *J. Chem. Phys.*, **56,** 2527 (1972).
Curry, F. E., and C. C. Michel, "A Fiber Matrix Model of Capillary Permeability," *Microvasc. Res.*, **20,** 96 (1980).
Deen, W. M., "Hindered Transport of Large Molecules in Liquid-Filled Pores," *AIChE J.*, **33,** 1409 (1987).
Durlofsky, L., and J. F. Brady, "Analysis of the Brinkman Equation as a Model for Flow in Porous Media," *Phys. Fluids,* **30,** 3329 (1987).
Ethier, C. R., "The Hydrodynamic Resistance of Hyaluronic Acid: Estimates from Sedimentation Studies," *Biorheols.*, **23,** 99 (1986).
Fanti, L., and E. Glandt, "Partitioning of Spherical Particles into Fibrous Matrices I," *J. Colloid Inter. Sci.*, in press (1989).
Finlayson, B. A., *Nonlinear Analysis in Chemical Engineering,* Ch. 4, McGraw-Hill, New York (1980).
Freed, K. F., and M. Muthukumar, "On the Stokes Problem for a Suspension of Spheres at Finite Concentrations," *J. Chem. Phys.*, **68,** 2088 (1978).
Hasimoto, H., "On the Periodic Fundamental Solutions of the Stokes Equations and their Application to Viscous Flow Past a Cubic Array of Spheres," *J. Fluid Mech.*, **5,** 317 (1959).

Hinch, E. J., "An Averaged-Equation Approach to Particle Interactions in a Fluid Suspension," *J. Fluid Mech.*, **83,** 695 (1977).
Howells, I. D., "Drag Due to the Motion of a Newtonian Fluid through a Sparse Random Array of Small Fixed Rigid Objects," *J. Fluid Mech.*, **64,** 449 (1974).
Jackson, G. W., and D. F. James, "The Permeability of Fibrous Porous Media," *Can. J. Chem. Eng.*, **64,** 364 (1986).
Jeffrey, D. J., and Y. Onishi, "Calculation of the Resistance and Mobility Functions for Two Unequal Rigid Spheres in Low-Reynolds-Number Flow," *J. Fluid Mech.*, **139,** 261 (1984).
Kim, S., and R. T. Mifflin, "The Resistance and Mobility Functions of Two Equal Spheres in Low-Reynolds-Number Flow," *Phys. Fluids,* **28,** 2033 (1985).
Koch, D. L., R. G. Cox, H. Brenner, and J. F. Brady, "The Effect of Order on Dispersion in Porous Media," *J. Fluid Mech.*, **200,** 173 (1989).
Laurent, T. C., I. Bjork, A. Pietruszkiewicz, and H. Persson, "On the Interaction between Polysaccharides and Other Macromolecules: II. The Transport of Globular Particles through Hyaluronic Acid Solutions," *Biochimica et Biophysica Acta,* **78,** 351 (1963).
Laurent, T. C., and A. Pietruszkiewicz, "The Effect of Hyaluronic Acid on the Sedimentation Rate of Other Substances," *Biochimica et Biophysica Acta,* **49,** 258 (1961).
Ogston, A. G., "The Spaces in a Uniform Random Suspension of Fibres," *Trans. Farad. Soc.*, **54,** 1754 (1958).
Ogston, A. G., B. N. Preston, and J. D. Wells, "On the Transport of Compact Particles through Solutions of Chain-Polymers," *Proc. R. Soc. Lond. A,* **333,** 297 (1973).
Peppas, N. A., and C. T. Reinhart, "Solute Diffusion in Swollen Membranes: I. A New Theory," *J. Membrane Sci.*, **15,** 275 (1983).
Phillips, R. J., J. F. Brady, and G. Bossis, "Hydrodynamic Transport Properties of Hard-Sphere Dispersions: I. Suspensions of Freely Mobile Particles," *Phys. Fluids,* **31,** 3462 (1988a).
——— "Hydrodynamic Transport Properties of Hard-Sphere Dispersions: II. Porous Media," *Phys. Fluids,* **31,** 3473 (1988b).
Spielman L., and S. L. Goren, "Model for Predicting Pressure Drop and Filtration Efficiency in Fibrous Media," *Envir. Sci. Tech.*, **2,** 279 (1968).

Manuscript received June 15, 1989, and revision received Sept. 6, 1989.